JOURNAL OF VIROLOGY, Aug. 2009, p. 7524–7535 Vol. 83, No. 15
0022-538X/09/$08.00+0 doi:10.1128/JVI.00429-09

Characterization of the Behavior of Functional Viral Genomes during the Early Steps of Human Immunodeficiency Virus Type 1 Infection▽

Vanessa Arfi,[1,2,3] Julia Lienard,[1,2,3] Xuan-Nhi Nguyen,[1,2,3] Gregory Berger,[1,2,3] Dominique Rigal,[4] Jean-Luc Darlix,[1,2,3] and Andrea Cimarelli[1,2,3]*

LaboRetro, Department of Human Virology, Ecole Normale Supérieure de Lyon, Lyon, France[1]; INSERM, U758, Lyon, France[2]; University of Lyon 1, IFR128 BioSciences Lyon-Gerland, Lyon-Biopole, Lyon, France[3]; and Etablissement Français du Sang, Lyon, France[4]

Received 27 February 2009/Accepted 13 May 2009

Infectious viral DNA constitutes only a small fraction of the total viral DNA produced during retroviral infection, and as such its exact behavior is largely unknown. In the present study, we characterized in detail functional viral DNA produced during the early steps of human immunodeficiency virus type 1 infection by analyzing systematically their kinetics of synthesis and integration in different target cells. In addition, we have compared the functional stability of viral nucleoprotein complexes arrested at their pre-reverse transcription state, and we have attempted to measure the kinetics of loss of capsid proteins from viral complexes through the susceptibility of the early phases of infection to cyclosporine, a known inhibitor of the interaction between viral capsid and cyclophilin A. Overall, our data suggest a model in which loss of capsid proteins from viral complexes and reverse transcription occur concomitantly and in which the susceptibility of target cells to infection results from a competition between the ability of the cellular environment to quickly destabilize viral nucleoprotein complexes and the capability of the virus to escape such targeting by engaging the reverse transcription reaction.

The early steps of infection by the human immunodeficiency type 1 retrovirus (HIV-1) are a complex series of events that begins with the engagement of cellular receptors by the viral envelope and the entry of the viral nucleoprotein core complex into the cytoplasm of target cells. This complex is composed of several viral and possibly cellular factors that form a shell around the viral RNA genome and chaperone it through reverse transcription and integration into the host genome, while assuring its protection from the cytoplasmic environment (12, 16).

Overall, the early steps of HIV-1 infection are a rather inefficient process in which a high proportion of viral particles penetrates the cytoplasm of target cells without resulting in an integrated provirus (2, 23). The reasons for this inefficiency are not known at present. In particular, it is not appreciated whether noninfectious viral particles serve as decoys, whether they result from defective assembly, or whether they are the consequence of the action of intracellular antiviral defenses.

In cells highly susceptible to HIV-1 infection, ratios as low as 1 infectious particle among 100 to 1,000 noninfectious particles have been evoked (2, 23, 40). However, a more recent study indicated that the majority of viral particles in these previous estimates do not enter target cells and that among those that do the infectious/noninfectious particle ratio is 1 out of 8 to 10 (46). These values describe the infection of established cell lines, generally highly susceptible to HIV-1 infection. However, most primary cells targeted by HIV-1 in vivo display a greater degree of resistance against HIV-1 and as a consequence the proportion of noninfectious viruses increases with their resistance toward HIV-1.

When the susceptibility of different cell types to HIV-1 infection is analyzed, it is clear that not only different cell types can overall be more or less permissive to HIV-1 infection, as primary blood lymphocytes (PBLs) versus macrophages for example, (15, 39), but that the same cell type can display substantial resistance or complete permissiveness to the virus according to its activation status, as is the case for quiescent versus activated PBLs (7, 15, 17, 25, 26, 29, 39, 51, 52, 56, 57). Given that these differences are independent from the entry pathway taken by the virus, as they are generally maintained upon infection with particles carrying wild-type and heterologous envelope proteins, they are likely to reflect the strong influence of the cytoplasmic environment on the different phases of HIV-1 infection (3, 46). Which are the reasons for the great variability in the susceptibility of target cells to infection? Which steps are influenced in different cell types?

A number of studies have addressed these issues and have linked delayed kinetics of reverse transcription and/or integration to a general resistance of target cells to infection (17, 25, 26, 29, 35, 48–51, 56, 57). This is the case, for example, for quiescent lymphocytes and nonstimulated blood monocytes in which the process of reverse transcription occurs in a matter of days rather than hours (3, 61). Similarly, the higher susceptibility of activated PBLs versus macrophages has been ascribed to faster kinetics of reverse transcript accumulation (15, 39, 42). In this particular case, the susceptibility to HIV-1 infection seems to correlate with the concentration of the intracellular deoxynucleoside triphosphate (dNTP) pool, implying that dNTPs may be a limiting factor during RT (39, 42). However, although the exogenous addition of dNTPs increases in some

* Corresponding author. Mailing address: LaboRetro, Department of Human Virology, ENS-Lyon INSERM, U758, 46 Allée d'Italie, 69364 Lyon, France. Phone: (33) 4 72728696. Fax: (33) 4 72728137. E-mail: acimarel@ens-lyon.fr.

▽ Published ahead of print on 20 May 2009.

instances the amount of viral DNA produced, this effect may be indirect (14, 27) and seems not to occur in all cell types (48), indicating that multiple factors contribute to the susceptibility of target cells to infection.

In the majority of previous reports, the study of the accumulation of viral DNA intermediates has been carried out by PCR (15, 18, 38, 39, 56). If this technique allows a general appreciation of the completion of reverse transcription as a whole, it cannot by its nature distinguish between infectious and noninfectious viral genomes. Given the relative disproportion between these two species, it is possible that the behavior of true infectious genomes is masked by the mass of noninfectious ones.

In the present study, we have studied in detail the behavior of infectious viral genomes of HIV-1 during the early steps of infection, defined here as viral genomes capable of stable expression of the viral coded *gfp* upon integration, as measured by flow cytometry analysis. We have determined a canvas of the early steps of infection by analyzing precisely a series of parameters that describe these phases such as the kinetics of viral DNA synthesis and that of integration. By performing infections in the presence of a reversible reverse transcriptase (RT) inhibitor, we have been able to arrest viral complexes at their pre-reverse transcription state and to determine their stability over time in a comparison among different cell types. Finally, we have attempted to characterize the process of capsid molecules loss from viral complexes, one of the features believed to be associated to uncoating through the measurement of the susceptibility of infection to cyclosporine (Cs), an inhibitor of the viral capsid (CA)-cyclophilin A (CypA) interaction. On this canvas of the early steps of viral infection, we have investigated the influence of the cytoskeleton, of the activation status of target cells and of the kinetics of viral DNA synthesis.

MATERIALS AND METHODS

Cells. Human PBLs and monocytes were obtained at the Etablissement Français du Sang de Lyon from the blood of healthy donors, as previously described (3). Monocytes were purified by two density gradient centrifugations using Ficoll and Percoll, followed by a negative selection procedure with MACS microbeads to obtain a population of purity greater than 95% (Miltenyi Biotec). Cells were maintained in RPMI 1640 medium, supplemented with 10% fetal calf serum and specified cytokines. Differentiated macrophages were obtained after incubation of monocytes for 4 to 6 days in granulocyte-macrophage colony-stimulating factor (R&D Systems). PBLs were stimulated for 12, 24, or 72 h with 1 μg of phytohemagglutinin (PHA; Sigma)/ml and 150 U of human recombinant interleukin-2 (IL-2; AIDS Reagent and Reference Program of the National Institutes of Health [NIH])/ml prior to infection. HeLaP4 fibroblasts (referred to as HeLa cells throughout the text, expressing CD4 and containing an integrated copy of β-galactosidase under the control of the viral long terminal repeat) or 293T cells were maintained in complete Dulbecco modified Eagle medium supplemented with 10% fetal calf serum.

Production and purification of viral particles. HIV-1-derived lentiviral vectors were produced by calcium phosphate DNA transfection of 293T cells with three plasmids: the packaging vector coding Gag-Pro-Pol and nonstructural viral proteins (8.2 [33]), the Env-coding construct, and the transfer vector coding a mini-viral genome expressing enhanced green fluorescent protein (GFP) under the control of the constitutive cytomegalovirus (CMV) promoter. Vectors were pseudotyped with the X4-tropic envelope PMA243 (AIDS Reagent and Reference Program of the NIH) or with the vesicular stomatitis virus G envelope protein (VSVg). At 48 h posttransfection, vectors were purified from the supernatant of transfected cells by ultracentrifugation through a 25% sucrose cushion, as previously described (22). Viral particles were then resuspended, and their infectious titer was determined on HeLaP4 cells after flow cytometry analysis. Control infections were routinely performed in the presence of RT inhibitors to exclude pseudotransduction (i.e., the appearance of GFP-positive cells due to GFP protein carryover, rather than to the de novo GFP synthesis after viral infection [34]).

As a control for lack of integration, a single point mutant in the integrase (IN) was used (D116A). This mutation is present within the catalytic site of the enzyme and results in an integration-defective virus (8, 32).

The Q151N RT mutant was engineered in the 8.2 vector by standard molecular biology techniques. This mutant has been previously described to exhibit low DNA polymerization rates (19).

Infections. To ensure the entry of no more than one infectious viral genome per cell, viral inputs that allowed infection of less than 30% of cells were used. These varied according to the target cell type and the donor but generally corresponded to a routine number of HeLa infectious units per cell (or multiplicities of infection [MOIs]) of 0.1, 1, and 5 for HeLa cells, PBLs, and macrophages, respectively. Infections were carried out for 1 h on 10^5 cells prior to virus removal and extensive cell washing, with the exception of Cs sensitivity assays in which infections were carried out for 30 min. Synchronization of infection or shorter incubation times did not modify the results obtained here (results not shown). Macrophages were used 4 to 5 days after differentiation, whereas PBLs were activated for the indicated amount of time with PHA/IL-2 prior to infection. Drugs were obtained as follows: the RT inhibitors nevirapine, efavirenz, aziolothymidine, and dideoxyinosine (used at 20 μg/ml; AIDS Reagent and Reference Program of the NIH); the diketo acid IN inhibitors 118-D-24, L-708,906, and L-731,988 (used at 20 μg/ml; AIDS Reagent and Reference Program of the NIH and kindly provided by J. F. Mouscadet, ENS-Cachan, Cachan, France); Cs (5 μM; Sigma); nocodazole and latrunculin B (Sigma; used at 1 μM and added from 30 min prior to infection to 23.5 h during infection for a total of 24 h prior to medium replacement). The percentage of GFP^+ cells was determined at 72 h postinfection by flow cytometry.

Half-times for the different parameters were calculated by plotting the values obtained for each curve using an Excel graphic program, and the standard deviations were calculated by using the Student *t* test.

To evaluate the existence of cell type-specific kinetic differences in drug uptake, the ability of the drugs used here to inhibit the RT and IN reactions shortly after their addition to the cells was determined. Cells (10^5 and 4×10^5, respectively) were incubated in the presence or absence of nevirapine or L-731,988, at 2 or 20 h after infection, respectively. At 30 min after incubation, the medium was removed, the cells were lysed, and the specific RT and IN activities determined in vitro. RT activity in cell lysates was determined with an exogenous RT reaction, a reaction in which the ability of RT to incorporate ^{32}P-labeled dTTP into a poly(rA)/oligo(dT) matrix is quantified (3). For IN activity, previously reported conditions were used (31). Briefly, cells were lysed in 20 mM Tris-Cl (pH 7.5)–5 mM $MgCl_2$–150 mM KCl–2 mM dithiothreitol–0.025% digitonin and centrifuged for 5 min at 2,000 rpm. The pellet was resuspended in the same buffer containing 0.25% digitonin and similarly centrifuged for 5 min at 2,000 rpm. The soluble fraction reported to contain most of the IN activity was incubated with an exogenous DNA template of 200 nucleotides obtained upon PCR amplification with primers AC65 and AC108 from a pEF/myc/cyto plasmid (Invitrogen). The ability of viral DNA to be integrated into this short template was assessed by PCR mimicking conditions used for AluPCR, i.e., using one primer specific for the 3′ viral long terminal repeat (AC37) and one specific for the template (AC108). Upon amplification, samples were transferred onto a nylon membrane by slot blot (Bio-Rad) and hybridized to an HIV-1 specific probe (AC34), and the signals were quantified by phosphorimager analysis. The RT and IN results shown here are within the linear range of detection of the assays (data not shown).

The primer sequences were as follows: AC37, CACTCCCAACGAAGAC AAG; AC34, TCCCAGGCTCAGATCTGGTCTAAC; AC65, GGAATTTGG CCTTTTTGAGTTTGG; and AC108, TAGAAGGCACAGTCGAGGCTG.

Immunofluorescence. HeLa cells were grown on coverslips and treated with nocodazole or latrunculin B (Sigma) for 30 min or 24 h before being fixed in 3% paraformaldehyde–phosphate-buffered saline, while PBLs and macrophages were centrifuged onto microscope slides with a cytospin. Free aldehydes were quenched with 5 mM NH_4Cl. Cells were then permeabilized with 0.2% Triton X-100 for 5 min and blocked for 15 min in 3% (wt/vol) bovine serum albumin–phosphate-buffered saline. After immunostaining, images were acquired on an Axiovert 100M Zeiss LSM 510 confocal microscope. Rhodamine-conjugated phalloidin and the anti-α tubulin antibody used here were from Sigma and Santa Cruz, respectively.

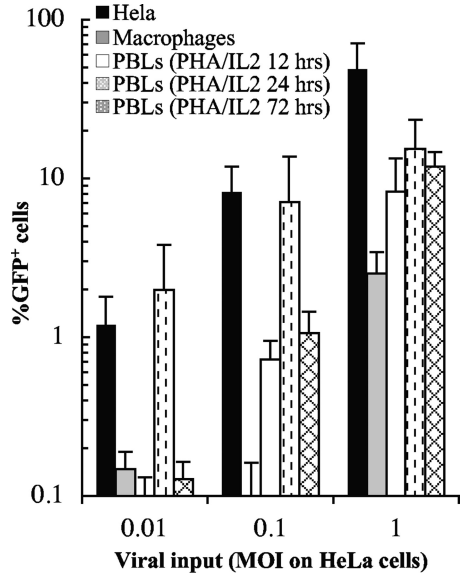

FIG. 1. Cell type-specific susceptibility during the early steps of HIV-1 infection. VSVg-pseudotyped CMV-GFP bearing HIV-1 lentiviral vectors was produced by transient transfection of 293T cells, purified by ultracentrifugation through a 25% sucrose cushion, and quantified. Identical numbers of HeLa infectious units per cell were used (MOIs as measured on HeLa cells) on the indicated cell types. The percentage of GFP^+ cells was measured 3 days postinfection by flow cytometry. PBLs were activated with PHA/IL-2 for the indicated amounts of time prior to infection. The results are representative of four independent experiments with cells obtained from distinct donors.

RESULTS

Cell type-specific susceptibility to HIV-1 infection and experimental set up. To directly compare the early phases of infection among different cell types, CMV-GFP-bearing HIV-1-derived lentiviral vectors pseudotyped with the pantropic VSVg were used. This setting neutralized potential differences among cell types with respect to viral entry (3) and proviral expression due to cellular receptors and viral promoter activities and allowed us to focus uniquely on events occurring between entry and integration.

First, we compared the different susceptibilities to infection of stimulated PBLs and differentiated macrophages in comparison with HeLa cells, a cell type highly susceptible to HIV-1 infection. Equal amounts of cells were infected with increasing viral inputs (MOIs as determined on HeLa cells), and the outcome of infection was determined 3 days later by flow cytometry (Fig. 1). Under these conditions, HeLa cells were highly permissive to HIV-1 infection similarly to PHA/IL-2-stimulated PBLs. We found that PBLs stimulated for 24 h with PHA/IL-2 prior to infection were more prone to HIV-1 infection than PBLs stimulated for shorter or longer time points. This was more evident at low than at high viral inputs. In contrast, infection of macrophages was close to the baseline levels for low viral inputs. Overall, the differences in infectivity ranged between 10- and 80-fold depending on the initial viral load. Given that VSVg mediates efficient viral entry in these cell types (3), these differences can be ascribed to the influence of the intracellular environment on the early steps of viral infection.

To identify the steps affected in each cell type and to potentially correlate them to the susceptibility of a given cell type to the early phases of HIV-1 infection, we decided to characterize these phases by determining four different parameters: the speed of reverse transcription and integration and the stability of viral nucleoprotein complexes, as well as the sensitivity of viral infection to incubation with Cs, a drug that targets the binding between CA and CypA and may thus provide a measure of uncoating through the loss of the effect of Cs during infection. The main goal of our analysis was the characterization of the behavior of functional viral genomes, that is, of the genomes capable of stable expression after integration, as assessed via the detection of the viral coded GFP by flow cytometry. This measure allowed us to focus solely on infectious viral genomes and not on the majority of noninfectious viral genomes that are a confounding factor in the study of these phases. These experiments were carried out using viral inputs that allowed the analysis of less than 1 infectious viral genome per cell, and this was achieved using viral inputs that yielded less than 30% of infected cells. The experimental scheme used is depicted in Fig. 2A. The kinetics of reverse transcription and integration were determined by the addition of appropriate inhibitors at different points postinfection and by determining the percentage of GFP-positive cells obtained 3 days postinfection (or at the estimated time for the IN inhibitor [see below]). Addition of antiviral drugs directed against RT or IN during infection will block either the completion of reverse transcription molecules or their integration. In the first case, viral DNA molecules will not establish infection (no GFP^+ cells). In the second, viral DNA molecules that fail to integrate may be transiently expressed from episomes but will be ultimately lost over cell division (early GFP^+ cells will thus become negative over time). On the other hand, the drugs will not affect viral DNA molecules that have been completed prior to their addition. Therefore, by plotting the normalized percentage of GFP^+ cells obtained at each time point, a kinetic curve can be obtained and a $t_{50\%}$ value, representing the time required to complete synthesis of half of the infectious viral DNA genomes, can be estimated.

A similar approach was used to obtain a measure of the functional stability of viral nucleoprotein complexes in their pre-reverse transcription state. Despite the fact that reverse transcription starts within virion particles, its extent is under normal conditions limited (60). In this respect, the pre-reverse transcription state defined here includes this limited viral DNA synthesis, that at least in intact virion particles does not induce appreciable morphological changes in viral cores (59). Infections were performed in the presence of a reversible RT inhibitor to freeze viral complexes in their pre-reverse transcription state and the drug was removed at different times postinfection to allow infection to resume. In this setting, only viral complexes that remained functionally stable will be able to resume and complete infection, while the rest, which may be degraded or brought to inappropriate places, will not. Thus, the curve obtained will represent the loss of infectivity of viral complexes arrested at their pre-reverse transcription state.

Nevirapine was selected as an RT inhibitor, because it is an efficient nonnucleoside RT inhibitor that binds its target directly and thus ought not to be influenced by fluctuations in the intracellular concentration of dNTPs (Fig. 2B) and because it

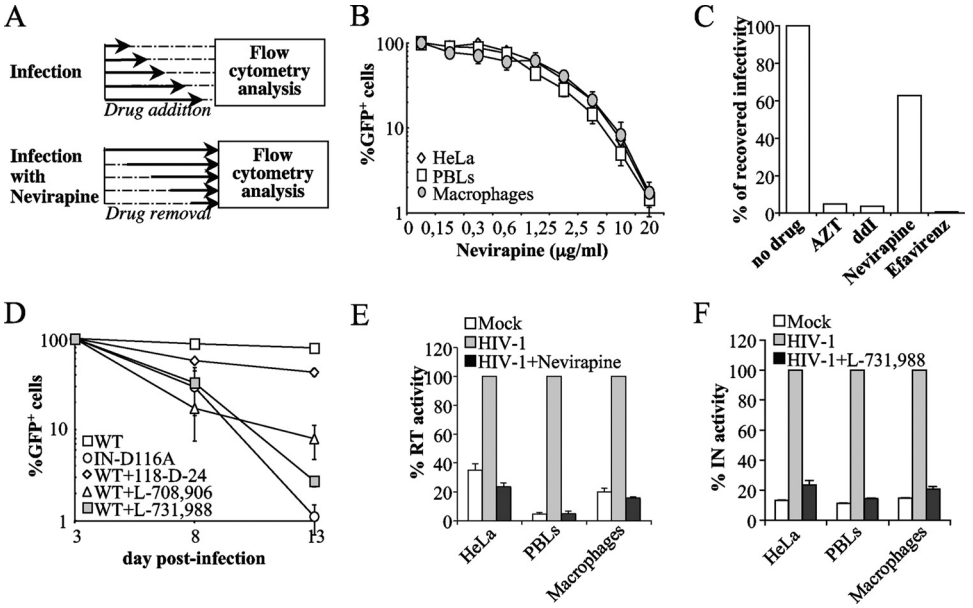

FIG. 2. Experimental setup. (A) Schematic approach used throughout the present study to determine the different parameters of HIV-1 infection. Arrows indicate the proceeding of infection, while dotted lines indicate the arrest of a particular step upon addition of antiviral compounds. Briefly, the speeds of reverse transcription, integration, and uncoating were determined by the addition of appropriate inhibitors (nevirapine, L-731,988, and Cs) at different times postinfection and by measuring the percentages of GFP-positive cells 3 days postinfection compared to control infections performed in the absence of drugs. To measure the stability of viral nucleoprotein complexes, a reverse approach was used in which infections were performed in the presence of a reversible RT inhibitor to freeze viral complexes at their pre-reverse transcription state. Upon drug removal at different times postinfection, complexes that have remained functional will resume infection, yielding GFP-positive cells. (B) To determine possible differences in the inhibitory concentrations of nevirapine among the different cell types used here, infections were performed in the presence of increasing drug concentrations. The efficacy of infection was determined 3 days later by flow cytometry. Normalized results from three independent experiments are shown. (C) To identify a reversible RT inhibitor, HeLa cells were infected for 2 h in the presence of the indicated drug at 20 μg/ml prior to drug removal by extensive cell washing. The percentage of infection was determined 3 days after by flow cytometry analysis. The graph presents data from a representative experiment. (D) To identify effective IN inhibitors, three different diketo acid IN inhibitors (118-D-24, L-708,906, and L-731,988 at 20 μg/ml) were used and compared to an integration defective HIV-1 mutant (IN D116A). HeLa cells were infected with wild-type (WT) HIV-1 in the presence of the indicated IN inhibitor or infected with the D116A mutant. The percentage of GFP^+ cells was determined at the indicated time postinfection to estimate the time required to lose GFP expression from episomal viral DNA. The graph presents normalized data obtained with three independent experiments. (E) To determine whether nevirapine entered rapidly in the different cell types used here, cells were either mock treated or infected for 2 h and then incubated for 30 min with nevirapine. Upon medium removal, cells were lysed, and cell lysates were tested in an exogenous RT reaction. The graph presents data obtained from two different donors. (F) Similar to panel E, cells infected for 20 h were incubated for 30 min with L-731,988 and then lysed. The ability of viral DNA to integrate into an exogenous DNA template was assessed by PCR using a primer specific for the viral DNA and one for the exogenous DNA template. The signals obtained after hybridization with a ^{32}P-labeled HIV-1-sepcific probe are shown here. The graph presents data from two donors.

is reversible. Indeed, when HeLa cells were infected for 2 h in the presence of several anti-RT drugs prior to extensive cell washing and drug removal, Nevirapine was found to be the best reversible compound (Fig. 2C). No GFP-positive cells were obtained if drugs were maintained throughout infection (data not shown).

To select an effective IN inhibitor, we compared several diketo acid compounds for their ability to inhibit wild-type HIV-1 infection compared to an integration-incompetent HIV-1 mutant (D116A). HeLa cells were infected and analyzed 3, 8, and 13 days postinfection (Fig. 2D). At 3 days postinfection, a substantial number of cells scored positive for GFP. Given that this was observed also after infection with the integration-deficient HIV-1 virus, this result indicates that the effect of antiviral compounds on integration may be masked by GFP expression from episomal DNA. Given that episomal DNA expression is transient (32, 41), we hypothesized that GFP expression would be diluted over cell division. Indeed, when infected cells were kept in culture and examined at longer times postinfection, the percentage of GFP-positive cells decreased over time in cells infected with the integration defective HIV-1 mutant but remained stable after infection with wild-type HIV-1. Of the three anti-IN compounds tested, the diketo acid inhibitor L-731,988 was selected for further use. Loss of GFP expression was accompanied by loss of viral DNA as assessed by PCR (results not shown). In addition to identifying an efficient IN inhibitor, these results indicate that the time required for loss of GFP expression from episomal viral DNA is of 13 days in HeLa cells and of 7 days in activated PBLs (not shown). As such, for the determination of the kinetics of integration, GFP^+ cells were analyzed at these indicated times. In the case of differentiated macrophages, episomal expression of GFP is stable due to the absence of cell division. However, this problem could be minimized, although not entirely eliminated (see the background level of GFP^+ cells obtained at early time points in macrophages [Fig. 3B]), by performing infections at low viral inputs. We believe this is probably due to lower rates of transcription from episomes in

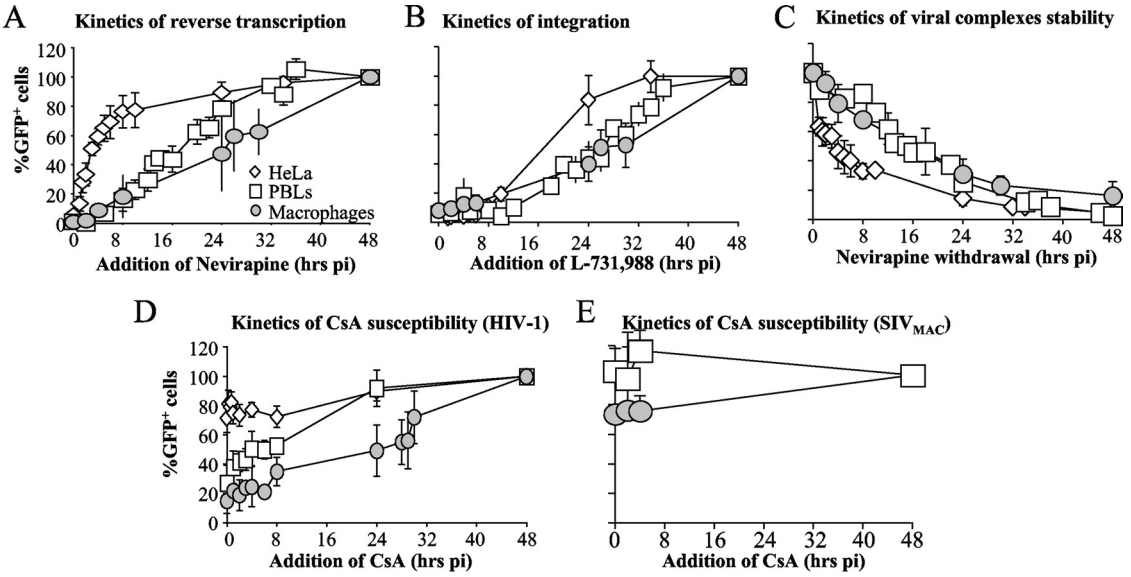

FIG. 3. Determination of the kinetics of infectious viral DNA synthesis, integration, viral nucleoprotein complex stability, and Cs susceptibility. HeLa cells, PBLs, and macrophages were infected for 1 h with VSVg-pseudotyped CMV-GFP-bearing HIV-1 vectors with viral inputs that allowed infection of less than 30% of target cells (to ensure the entry of less than 1 infectious viral genome per cell). Within this range, fluctuations in the percentage of infected cells did not modify the results depicted here. The kinetics of reverse transcription (A), integration (B), viral nucleoprotein complex stability (C), and susceptibility to Cs (CsA) (D and E) were determined by using the scheme depicted in Fig. 2A. The percentage of GFP^+ cells obtained at each time point after flow cytometry analysis 3 days postinfection was normalized to infections performed in the absence of nevirapine. The graph presents data obtained from seven to eight independent experiments and donors.

this cell type. Of note, in all of the remaining kinetics, similar results were obtained if cells were analyzed at 3 or 13 days postinfection, indicating that episomal expression plays a marginal role during wild-type integration-competent infection under the experimental conditions used here.

To determine the existence of possible differences in drug uptake among the different cell types used here, we determined the ability of nevirapine and of L-731,988 to inhibit RT and IN enzymatic activities shortly upon their addition on cells undergoing infection. For RT, cells were infected for 2 h as described above and then incubated with or without nevirapine for 30 min. Upon medium removal, cells were lysed and the RT activity in cellular lysates was measured via an exogenous RT reaction (Fig. 2E). Under these conditions, Nevirapine inhibited RT activity to baseline levels in all cell types, indicating that the drug is rapidly and actively absorbed. A similar approach was used to assess IN activity. Cells were incubated for 30 min with L-731,988, 20 h postinfection prior to medium removal and cell lysis. Upon preintegration complex enrichment, the ability of viral DNA to be integrated into an exogenous DNA substrate was evaluated by using a PCR approach equivalent to AluPCR, using one primer specific for viral DNA and one specific for the exogenous DNA substrate. Under these conditions, a short incubation with L-731,988 is sufficient to inhibit IN activity to baseline, indicating rapid drug uptake in target cells (Fig. 2F).

Kinetics of infectious viral DNA synthesis, integration and viral nucleoprotein complexes stability. Using the scheme depicted in Fig. 2A, the kinetics of functional reverse transcript accumulation was examined first (Fig. 3A). In HeLa cells, viral DNA synthesis proceeded very rapidly, and up to 80% of infectious viral genomes were completed within the first 8 h of infection. The remaining 20% accumulated at a slower pace, linearly until 48 h (Fig. 3A, $t_{RT50\%} = 3.7 \pm 1.2$ h). Not unexpectedly, reverse transcription proceeded more slowly in PBLs that had been activated with PHA/IL-2 for 24 h prior to infection and even more so in macrophages ($t_{RT50\%} = 16.5 \pm 1.4$ h and 24.2 ± 7.7 h, respectively). In the latter cell type, values displayed a substantial donor-specific variability. We have been thus far unable to correlate this variability with specific changes in the differentiation or maturation status of macrophages. PBLs activated with PHA/IL-2 behaved as PBLs activated with anti-CD3 and anti-CD28 antibodies plus IL-2 (data not shown). Similar results where obtained when aziolothymioline and dideoxyinosine were used in place of nevirapine, and no changes in the percentage of infected cells were observed if flow cytometry analysis was postponed until day 13 after infection, indicating that episomal expression of GFP is not a confounding issue in the analysis of the kinetics of reverse transcription (results not shown).

The kinetics of integration was then examined by using an identical experimental approach. In this case, given the presence of GFP expression from episomal DNA, the percentage of GFP^+ cells was determined by flow cytometry after the time required for loss of episomal GFP expression (Fig. 3B). The first events of integration started to be detectable by 8 h postinfection in HeLa cells, and the proportion increased steadily thereafter in all cell types ($t_{IN50\%} = 16.3 \pm 1.8$ h, $t_{IN50\%} = 25.1 \pm 3.2$ h, and $t_{IN50\%} = 26.7 \pm 5.8$ h, for HeLa cells, PBLs, and macrophages, respectively). The low level of GFP-positive cells found for early time points in macrophages can be ascribed to residual episomal expression of GFP. The kinetics of integration appeared overall more rapid in HeLa cells. However, it should be noticed that the delay observed between the

TABLE 1. Summary of the values obtained in this study

Cell type	Mean time (h) ± SD[a]				$\Delta_{RT\text{-}IN}$
	$t_{RT50\%}$	$t_{IN50\%}$	$t_{Stab50\%}$	$t_{Uncoat50\%}$[b]	
HeLa	3.7 ± 1.2[C]	16.3 ± 1.8[D]	3.8 ± 1.2	ND	12.6
PBLs (24 h)	16.5 ± 1.4[A]	25.1 ± 3.2[B]	16.2 ± 3.3	12 ± 2.8	8.6
PBLs (12 h)	26 ± 2.8	33 ± 1.9	24.6 ± 1.1	15.5 ± 4.6	7
PBLs (72 h)	10.5 ± 2.7	17.6 ± 1.9	5.16 ± 3.2	6.5 ± 1.4	7.1
Macrophages	24.2 ± 7.7	26.7 ± 5.8	16.6 ± 1.4	24.7 ± 6	2.5
PBLs (nocodazole)	25 ± 5	32 ± 2.5	ND	ND	7
HeLa (nocodazole)	4.6 ± 0.2	15.2 ± 0.2	ND	ND	10.6
HeLa (X4)	5.6 ± 2.3[C]	17.5 ± 0.5[D]	3.5 ± 0.5	ND	11.9
PBLs (X4)	15 ± 0.4[A]	27.3 ± 4.49[B]	12.6 ± 4	15 ± 0.7	12.3

[a] Identical superscript capital letters indicate paired conditions that display a P of >0.05 (Student t test). ND, not determined.
[b] $t_{50\%}$, the mid values between those obtained at t_0 and the 100% value obtained at t_{48}. Uncoating is measured here based on the susceptibility to Cs.

completion of viral DNA synthesis and integration was actually longer in HeLa cells than in the other cell types (Fig. 3A and see Table 1).

Next, the functional stability of viral nucleoprotein complexes in their pre-reverse transcription state was determined by measuring the percentage of GFP^+ cells recovered after removal of nevirapine at different times postinfection with respect to control infections performed in the absence of drug (Fig. 3C). In HeLa cells, a short incubation with nevirapine was sufficient to inactivate rapidly the vast majority of viral complexes ($t_{Stab50\%}$ = 3.8 ± 1.2 h), indicating that in their pre-reverse transcription conformation, viral nucleoprotein complexes are rapidly inactivated. On the other hand, slower and rather similar viral complex stabilities were observed in activated PBLs and differentiated macrophages ($t_{Stab50\%}$ = 16.2 ± 3.3 h and 16.6 ± 1.4 h, respectively).

Kinetics of Cs susceptibility in the early stages of viral infection. Uncoating remains a poorly understood process in which components of viral nucleoprotein complexes are progressively shed from the viral genome (5, 6, 37, 45). The major component lost during this phase appears the CA, which is in turn bound to the cellular cofactor CypA (9, 28, 31, 36). CypA-CA interaction enhances HIV-1 replication, and this positive effect on infectivity is counteracted by Cs by what seems a direct competition mechanism (44, 47). Although the exact mechanism through which CA and CypA favor HIV infection remains somewhat unclear and the relationship between Cs, CypA, and HIV may be multifactorial (1, 20, 54, 55), we have decided to use the susceptibility of HIV-1 infection to Cs over time as a measure—albeit indirect—of the loss of CA from viral complexes, a process generally defined as uncoating ($t_{Uncoat50\%}$). Indeed, the shedding of CA observed during viral nucleoprotein complexes rearrangement ought to protect HIV from the negative effect of Cs on infection. The kinetics of susceptibility to Cs was measured using a experimental approach similar to the one described above by adding Cs at different times postinfection and by evaluating the percentage of GFP^+ cells obtained 3 days postinfection by flow cytometry (Fig. 3D). Under these conditions, Cs had little to no effect (<2-fold) during HIV-1 infection of HeLa cells. Despite our efforts, we could not reliably measure a further decrease in HIV-1 infectivity in the presence of Cs in HeLa cells even when infections were performed for very short times (5 min [data not shown]). This may suggest that uncoating occurs within minutes after viral entry in this cell type. However, given that preincubation of HeLa cells with Cs prior to infection yields similar results (data not shown), it is also possible that the levels of CypA may be too elevated to be effectively inhibited in this cell type or that VSVg-mediated entry masks minor defects specifically in this cell type, as indicated by previous reports (1, 20, 54, 55). Instead, three- to fivefold infectivity defects were observed in activated PBLs and macrophages, respectively. This infectivity defect was slowly lost over time, albeit with cell type-specific differences ($t_{Uncoat50\%}$ = 12 ± 2.8 and 24.7 ± 6 h, respectively). Interestingly, when similar experiments were performed on PBLs and macrophages infected with SIV_{MAC} that does not require CypA for infection, minimal to no effects were observed (Fig. 3E). These results suggest that the effects observed here are largely dependent on the specific interaction between CA and CypA.

Effect of the viral entry pathway on the kinetic parameters of HIV-1 infection. Having established a canvas for the main steps of the early phases of viral infection, we sought to determine whether certain conditions could affect them. To this end, we sought to determine whether the viral entry pathway could influence downstream phases of infection. Vectors were pseudotyped with an X4-tropic Env (PMA243) and used to infect HeLa cells that express CD4 and CXCR4, as well as PBLs (Fig. 4, as indicated). The values of reverse transcription, integration, Cs susceptibility, and the stability of viral nucleoprotein complexes were similar to those obtained with VSVg pseudotyped particles, although a slightly longer delay seemed to elapse between the end of reverse transcription and integration. These differences however were not statistically significant (see Table 1). On the other hand, X4-tropic viruses seemed to display a slightly different susceptibility to Cs. Indeed, Cs exerted a small but reproducible positive effect on infectivity when added at early time points after infection of HeLa cells, whereas it decreased it twofold more than for VSVg viruses under similar conditions in PBLs.

Influence of cytoskeleton inhibitors on the early steps of HIV-1 infection. Components of the cytoskeleton have been associated with viral nucleoprotein complex migration to the nucleus in several studies. However, this association was mostly put in evidence by confocal microscopy, and few functional data exist on the effect of cytoskeleton disruption on the early steps of infection by cell-free HIV-1 (4, 11, 30). In light of the high disproportion between infectious and noninfectious viral

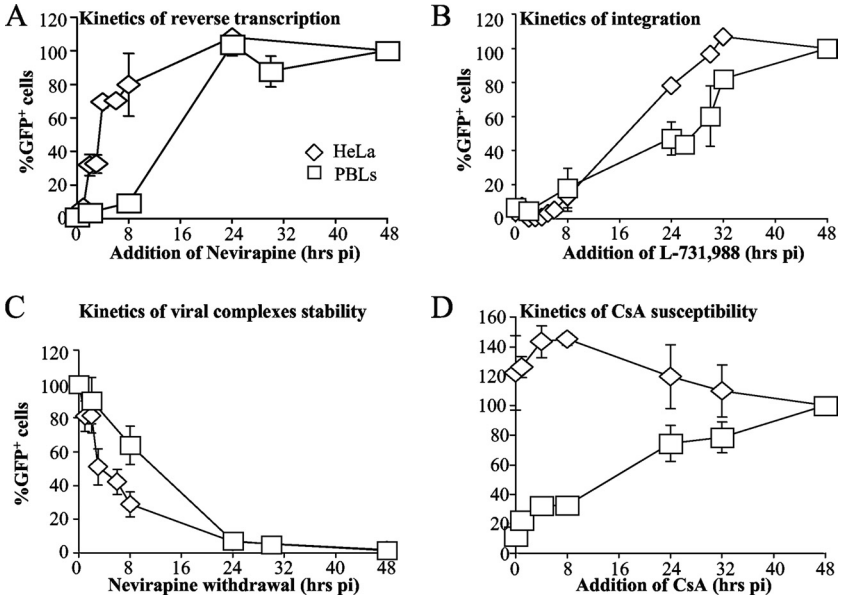

FIG. 4. Effect of viral entry on the kinetic parameters of infection. X4-pseudotyped virions were produced by cotransfection of 293T cells and tested on target HeLaP4 cells (HeLa in the text and figure) and PBLs stimulated for 24 h with PHA/IL-2 prior to infection. The kinetics of reverse transcription (A), integration (B), viral nucleoprotein complex stability (C), and Cs (CsA) susceptibility (D) were determined by using the scheme depicted in Fig. 2A. The graphs present results obtained from at least three independent experiments.

nucleoprotein complexes present during infection, we decided to address this issue by examining the effect of cytoskeleton inhibitors on the kinetic parameters determined here.

First, we determined the overall effect of cytoskeleton inhibitors on HIV-1 infectivity. Cells were treated with nocodazole or latrunculin B (inhibitors of microtubule and actin filaments dynamics, respectively) for 30 min prior to infection and through viral infection for a total of 24 h. After this time, toxic effects started to be clearly observed in treated cells and were thus avoided. Cells were either processed for confocal microscopy analysis or kept for a total of 3 days for flow cytometry analysis. As expected, nocodazole and latrunculin B treatment affected the cell cytoskeleton (Fig. 5A). However, when infections were performed in the presence of these drugs, the overall effect on infectivity was mild at best, and this occurred independently of the entry pathway (Fig. 5B). In the case of VSVg-HIV-1, nocodazole treatment had no effect on viral infectivity except for a reproducible three- to fourfold defect in PBLs. In contrast, latrunculin B treatment exerted a small but reproducible positive effect on the infection of HeLa cells and PBLs and a small negative effect in macrophages (<2-fold). In the case of X4-HIV-1, a twofold decrease in infectivity was observed in HeLa cells when infections were performed in the presence of nocodazole and latrunculin B, and a small but reproducible positive effect was observed in PBLs treated with nocodazole. To more finely characterize the effect of cytoskeleton inhibitors on the kinetic parameters of HIV-1 infection, the speeds of reverse transcription and integration were measured in cells where the effect was more appreciable (activated PBLs treated with nocodazole and infected with VSVg–HIV-1) compared to HeLa cells. Under these conditions, a clear delay in the speed of reverse transcription was observed in nocodazole-treated PBLs compared to untreated PBLs (of 8.5 h, $t_{RT50\%} = 25 \pm 5$ h, Fig. 5C). A similar delay was also observed in the speed of integration in PBLs ($t_{IN50\%} = 32 \pm 2.5$ h in PBLs, Fig. 5D). In contrast, no delay was observed in HeLa cells in which nocodazole displayed no effect on viral infectivity.

Effect of cellular activation on the early steps of infection. The status of cellular activation clearly influences the outcome of HIV-1 infection. To determine which parameters were specifically affected, PHA/IL-2-PBLs stimulated for 24 h were compared to PBLs stimulated for shorter and longer times prior to infection (12 and 72 h). A direct correlation was observed between the length of cell stimulation and the speed of several parameters of the early phases of HIV infection. In particular, when PBLs were activated for 12 h prior to infection, the first measurable events of completion of viral DNA molecules occurred after 16 h postinfection and increased steadily afterward (Fig. 6A). Instead, in PBLs activated for 24 and 72 h postinfection, a measurable amount of viral DNA molecules was completed within 4 to 8 h, and this amount increased linearly, albeit faster for PBLs stimulated 72 h prior to infection ($t_{RT50\%} = 26 \pm 2.8$ h and 10.5 ± 2.7 h after 12 and 72 h of stimulation, respectively). Similarly, integration occurred faster in PBLs activated for 72 h and was gradually slower in PBLs activated for 24 and 12 h (Fig. 6B, $t_{IN50\%} = 33 \pm 1.9$ h and 17.6 ± 1.9 h after 12 and 72 h of stimulation, respectively). Interestingly, despite the fact that the speed of reverse transcription varied, a delay of 7 ± 1.5 h was maintained in all cases with integration.

The loss of viral nucleoprotein complex functionality seemed directly proportional to the activation status of target PBLs (Fig. 6C). In PBLs stimulated for 72 h prior to infection, viral complexes arrested at their pre-reverse transcription state underwent a rapid loss of functionality that approximated the one observed in HeLa cells ($t_{Stab50\%} = 5.1 \pm 3.2$ h). Instead,

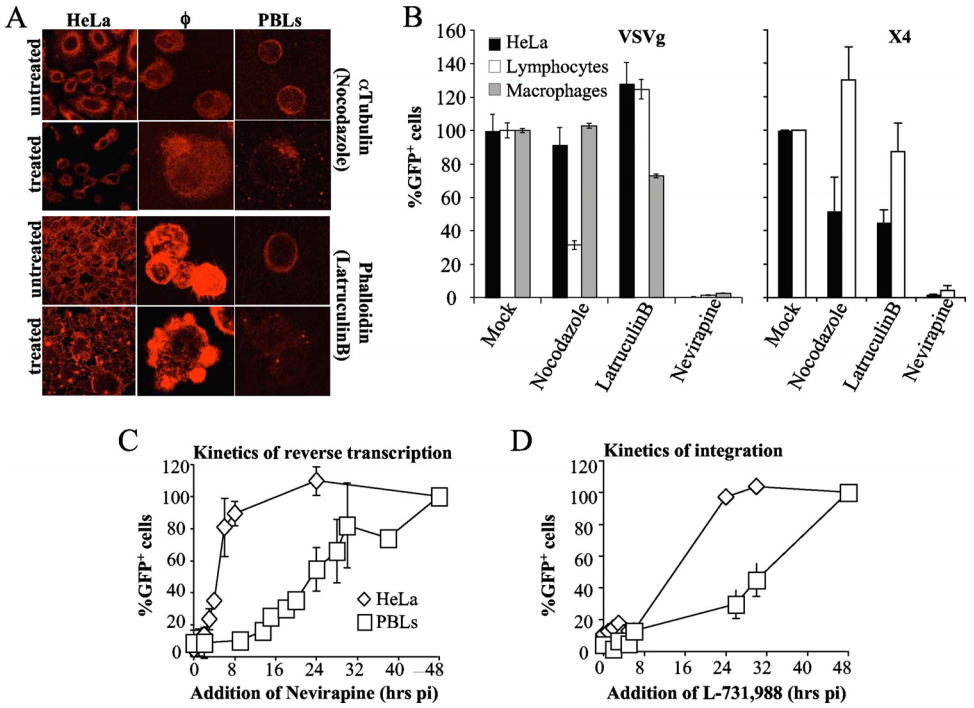

FIG. 5. Effect of cytoskeleton inhibitors on the early steps of viral infection. (A) HeLa cells, PBLs and macrophages were incubated with nocodazole or latrunculin B (1 μM) and analyzed by confocal microscopy 24 h later upon staining with an anti-α-tubulin antibody and fluorescently labeled phalloidin. Representative fields are shown. (B) To determine the effect of these drugs on the efficiency of viral infection, HeLa cells were treated or not with drugs for 30 min prior to infection, during 1 h of infection with HIV-1 wild-type virus, and then after the removal of the virus for a total of 24 h. The percentages of infected GFP-positive cells after infection with VSVg- and X4-pseudotyped viruses were determined at 3 days postinfection by flow cytometry and are here presented after normalization to mock-treated infections. (C and D) The kinetics of reverse transcription (C) and integration (D) were then determined. Given that the results obtained in the absence of drug were identical to those shown in Fig. 3, only findings obtained in its presence are displayed. The graphs present data obtained in three to five independent experiments with cells obtained from different blood donors.

viral complexes seemed more stable in cells that had been stimulated for only 12 h ($t_{Stab50\%}$ = 24.6 ± 1.1 h).

Incubation with Cs yielded a three- to fivefold defect in infectivity, and the defect was more pronounced in PBLs that had been stimulated for 12 h (Fig. 6D). In PBLs stimulated for longer times, sensitivity to Cs was lost rapidly within the first 8 h postinfection, while similar slopes of susceptibility to Cs were obtained in PBLs stimulated for 12 versus 24 h ($t_{Uncoat50\%}$ = 15.5 ± 4.6 h and 6.5 ± 1.4 h after 12 and 72 h of stimulation, respectively).

Relationship between reverse transcription and the remaining parameters of HIV-1 infection. To determine how the speed of reverse transcription influenced other events during viral infection, we characterized an RT mutant exhibiting low polymerization rates (Q151N [19]). This mutation impaired viral infectivity by 200-fold in HeLa cells, and we were unable to use it on primary cells, most probably due to its low infectivity (data not shown). For this reason, the Q151N mutant was analyzed only on HeLa cells.

As expected, the Q151N RT mutant virus displayed a considerable delay in the speed of reverse transcription compared to the wild type (Fig. 7A, $t_{RT50\%}$ 14.1 ± 1.4 h). Integration of the Q151N RT mutant virus was also delayed with respect to the wild type (by 4 h), although this delay was not as pronounced as in the case of reverse transcription (Fig. 7B, $t_{IN50\%}$ 20.6 ± 3.3 h).

Only minor changes were observed with respect to the functional stability of viral nucleoprotein complexes arrested at their pre-reverse transcription state (Fig. 7C, $t_{Stab50\%}$ = 3.74 ± 1.3 h), as expected if this parameter is governed by the intracellular environment. Finally, a clear, albeit small, effect of Cs was observed upon infection of HeLa cells with the Q151N RT mutant virus (2-fold, Fig. 7D). This is clearly different from the lack of effect of the same drug during infection of HeLa cells with wild-type virus.

Relationship between reverse transcription and the kinetics of susceptibility of HIV-1 infection to Cs. What is the relationship between uncoating and reverse transcription? This question remains difficult to tackle due to our poor knowledge of the uncoating process. We tried to address this question by examining the relationship between the reverse transcription process and the susceptibility of infection to Cs. To this end, we made use of the parameters measured above, and we have used wild-type VSVg-HIV-1 on PBLs stimulated for 24 h with PHA/IL-2 prior to infection. These cells were chosen since they can be well infected and because Cs clearly affects viral infection. Infections were carried out in the presence of nevirapine for 14 h, a time frame in which about half of the viral nucleoprotein complexes has been functionally destabilized. Then, after nevirapine removal, the kinetics of Cs susceptibility were determined. In this setting, if the loss of viral CA precedes or occurs independently of reverse transcription, infec-

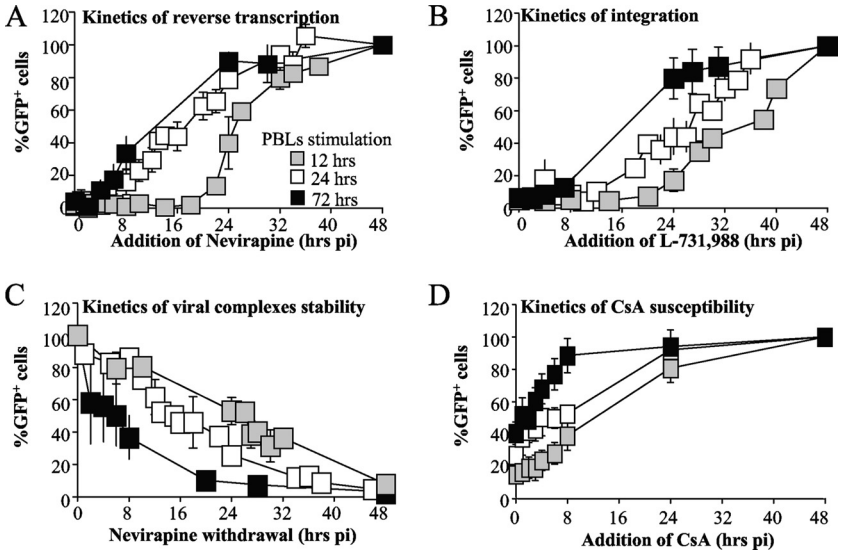

FIG. 6. Effect of lymphocyte activation on the early steps of infection. PBLs were stimulated for shorter and longer periods of time with PHA/IL-2 prior to infection (12 and 72 h) to modulate the levels of cellular activation, and results were compared to those obtained after stimulation for 24 h. The kinetics of reverse transcription (A), integration (B), viral nucleoprotein complex stability (C), and Cs (CsA) susceptibility (D) were determined by using the scheme depicted in Fig. 2A. The graphs present data obtained from three to six independent donors.

tion should not be susceptible to Cs (because at this time point, Cs exerts a minimal effect on infection; <2-fold [compare with Fig. 3D]). On the contrary, if reverse transcription is required for the loss of CA, infections ought to remain as sensitive to Cs as infections carried out in the absence of nevirapine. Our results indicate that, upon removal of nevirapine, infections remain sensitive to Cs, indicating that reverse transcription controls the susceptibility of viral infection to Cs (Fig. 8, compare to Fig. 3D).

DISCUSSION

In this study, we characterized the behavior of infectious HIV-1 genomes in a close comparison among different cell types. Our results reveal specific cell type differences with respect to all of the parameters analyzed here that converge in a general canvas of the early steps of HIV-1 infection.

Not unexpectedly, our results indicate that reverse transcription proceeds faster in HeLa cells and progressively slower in

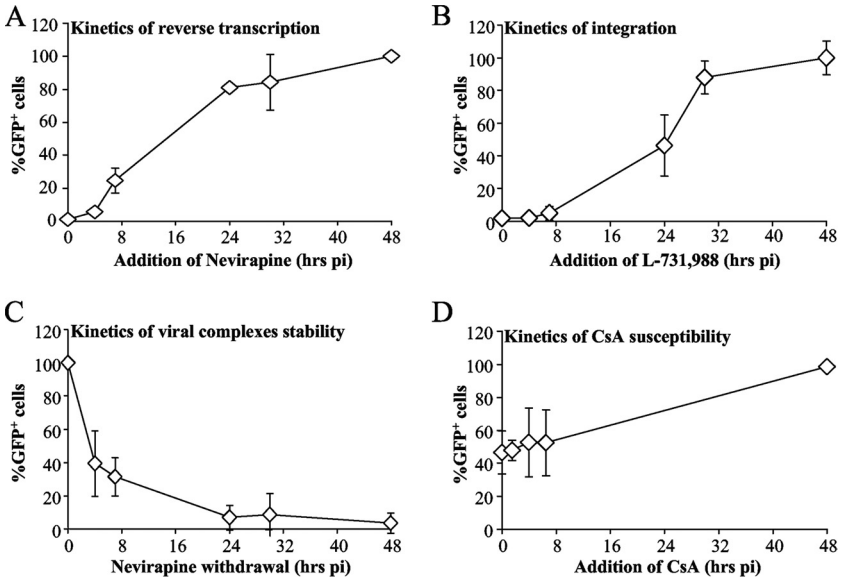

FIG. 7. Impact of slower reverse transcription kinetics on the remaining steps of HIV-1 infection. HeLa cells were infected with a single point mutant in HIV-1 RT (Q151N) previously characterized to display a delayed reverse transcription polymerization rate. The effect of this mutation on the different parameters determined above was then determined during infection of HeLa cells: (A) reverse transcription, (B) integration, (C) functional viral complexes stability, and (D) Cs (CsA) susceptibility. The graphs present results obtained from three to four independent experiments.

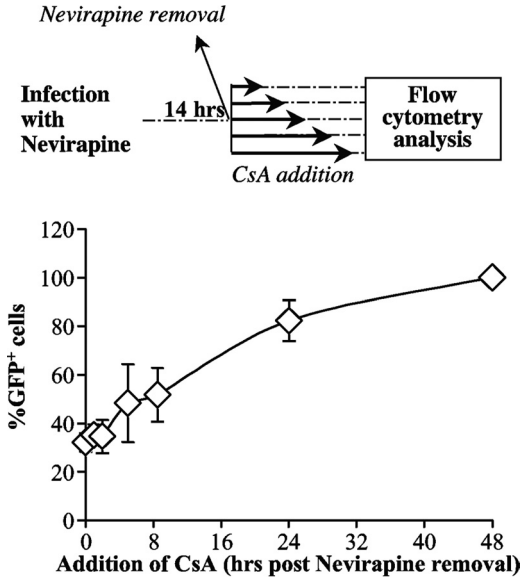

FIG. 8. Relationship between reverse transcription and susceptibility to Cs. PBLs activated for 24 h with PHA/IL-2 were infected with wild-type VSVg-HIV-1 in the presence of nevirapine for 14 h and then, after nevirapine removal, the susceptibility of viral complexes to Cs was assayed by the timely addition of Cs: t_0 indicates the time at which nevirapine was removed. The graph presents data obtained with cells derived from three different donors.

PBLs and macrophages. This conclusion has been reached before after studies that relied on PCR. However, our analysis adds novel and important information to these reports. Despite being variable, previous studies agreed in indicating a rapid accumulation of viral DNA up to the first 12 h after the infection of established cell lines (MT4, 293T, and HeLa). These values were generally found to be slower in PBLs and macrophages, peaking at around 24 and 48 h, with no major differences due to the entry pathway (7, 15, 39, 49, 50, 56). Subsequently, the overall amount of vDNA has been reported to decline, possibly as a result of increased degradation over time (18, 46).

Within the mixture of infectious and noninfectious vDNA produced after viral entry, our results suggest that infectious viral DNA genomes may accumulate faster than previously estimated, as in, for example, HeLa cells, where they are mostly completed by 8 h postinfection. This result is important since it may imply that one major determinant of the infectivity of viral genomes (meant as their ability to integrate) may be the speed at which they are synthesized. We favor this possibility because genomes produced early after viral entry may stand a better chance to avoid a mounting response from the cytoplasmic environment than those synthesized later. At present, the very presence of such antiviral responses remains to be fully explored. However, the decrease in the amount of vDNA observed after peak accumulation has been linked to proteasomal activity and interestingly, several components of the ubiquitin machinery have been implicated in the regulation of HIV-1 infection (10, 24). Whether this is part of a coordinated antiviral response or whether it impacts viral infection indirectly remains to be ascertained.

If at a first glance the speed of reverse transcription may be the major correlate for the susceptibility of target cells to HIV-1 infection, the results obtained here indicate that the stability of viral complexes also influences the outcome of infection. This parameter measures the ability of viral nucleoprotein complexes to retain their functionality after being arrested for different times postinfection at their pre-reverse transcription state (or at the initial stages of RT if the process started in intact viral particles) (60). Given that the values obtained vary greatly among cell types but remain constant within the same cell type for different mutants (as for example, in the case of the wild type versus the Q151N RT mutant), we believe that this parameter measures the influence of the cellular environment on viral complexes, an influence that may be exerted through their inappropriate trafficking or through the degradation of one or more of their components. At present, pilot experiments carried out in the presence of proteasome inhibitors seem to exclude a major role of the proteasome in viral nucleoprotein complexes stability (data not shown) despite the fact that proteasome inhibitors have been reported to exert a positive effect on HIV-1 infectivity (43). It is thus possible that the proteasome intervenes at other steps during the early phases of infection.

One possible model that integrates both the speed of reverse transcription and viral complex stability is that, upon entry, viral nucleoprotein complexes are subjected to two opposite influences: the negative influence of the cellular environment, measured here as their functional stability, and the protective effect of reverse transcription on viral complexes. The successful infection of a given cell type will depend on a balance between these two parameters.

In line with this model, the rapid inactivation of pre-reverse transcription viral complexes observed in HeLa cells may be compensated for by the protective effect of a rapid kinetics of reverse transcription, resulting in their high susceptibility to HIV-1. Macrophages may be less susceptible to HIV-1 than 12-h PBLs because, despite similar values of reverse transcription kinetics, viral complexes are more rapidly destabilized and, similarly, 72-h PBLs may not be more susceptible to infection than 24-h PBLs because, despite a faster kinetic of reverse transcription, viral complexes lose their functionality more rapidly.

The protective role of reverse transcription on viral complexes' stability may be achieved by promoting their migration toward favorable intracellular locations or through the induction of structural changes. We tend to favor this last possibility, since it is well established that viral nucleoprotein complexes undergo profound structural changes as the viral genome is transformed from single-stranded RNA to double-stranded DNA (21, 36). If cytoplasmic effectors recognize viral complexes by one of their components, they may lose this ability once this component is shed from the complex. Thus, by promoting such changes, reverse transcription may protect viral complexes from cytoplasmic effectors.

In the present study, we have used the susceptibility of HIV-1 to Cs as a measure of loss of CA from viral nucleoprotein complexes, a process generally defined as uncoating. Although results in the literature support this hypothesis since pharmacological disruption of the CA-CypA interaction affects infection through interference with the normal functions of CA and CA is progressively lost from viral complexes during in-

fection, the exact function played by CA-CypA has not been clearly defined and may be influenced by several parameters such as the viral entry pathway, the cellular expression levels of CypA, or an indirect effect on target cell physiology. Our results seem to exclude both the entry pathway, with the possible exception of HeLa cells, and an indirect effect on target cells since SIV_{MAC} infection is not affected by incubation with Cs. However, the possible complex nature of the relationship between CA and CypA may constitute a caveat in establishing a direct link between Cs susceptibility and CA loss, in other words, uncoating. We found that, apart from HeLa cells, which may constitute a peculiar exception, infection of both PBLs and macrophages is sensitive to Cs; this susceptibility is gradually lost over time and is specific to HIV-1 since it is not observed in the case of SIV_{MAC} infection. If our hypothesis is correct, our results indicate that the loss of viral CA from nucleoprotein complexes occurs concomitantly with reverse transcription and is prolonged over time in most primary cells. This supports the notion that uncoating occurs together with, but not after, reverse transcription, as recently proposed (5). It also suggests that some CA remains associated to viral complexes throughout the completion of the cycle, where it can exert different roles, perhaps including nuclear import or trafficking. This observation may also provide an explanation for the relatively late effects (after RT completion but prior to integration) observed upon targeting of HIV-1 CA with a TRIM-CypA fusion protein (53), a phenomenon that can hardly be explained if all CA has come off viral capsids.

Second, our study reveals a rather constant delay between the completion of reverse transcription and integration that appears cell type dependent. This is more apparent in PBLs activated from different times prior to infection or treated with cytoskeleton inhibitors. We do not know whether this delay is due to migration toward the nucleus, nuclear import per se, or even to events occurring after nuclear migration. Interestingly, this delay appears longer in HeLa cells and smaller in macrophages despite rather similar cellular sizes. These differences may reveal cell specific migration patterns leading to integration and suggest that in HeLa cells a long pause exists between the completion of reverse transcription and integration that is not observed in primary cell targets of HIV-1.

Finally, our results indicate that the early steps of HIV-1 infection may be achieved in the presence of an impaired cytoskeleton, since specific inhibitors exert only mild defects on the overall efficacy of infection. These results seem at odd with previous reports suggesting a role for the cytoskeleton in the intracellular migration of viral components toward the nucleus after infection with cell-free virus (5, 30, 58). However, these two sets of results cannot be compared directly. Indeed, previous studies posed the accent on migratory pathways of viral components by confocal microscopy without inherent discrimination between functional and nonfunctional complexes, while we focused uniquely on the gross functional impact of cytoskeleton-targeting drugs on infection. Most importantly, the time scale of these assays is bound to be different due to experimental constraints (minutes versus 24 h). It is thus possible that, in the presence of cytoskeleton perturbations, viral nucleoprotein complexes may quickly adapt to other pathways to attain the nucleus, and it is also likely that prolonged incubation with cytoskeleton inhibitors (required to observe the minimal effect described here) may in turn promote the formation of stress structures that the virus may use. We found that cytoskeleton deregulation slows reverse transcription, similar to what was has been reported previously (13), and we show here that this delay is passed on to integration. We have ignored at present whether this defect is direct or indirect.

Overall, our data are consistent with a model in which uncoating and reverse transcription occur concomitantly and in which the susceptibility of target cells to infection depends on a balance between the ability of the intracellular milieu to functionally destabilize viral nucleoprotein complexes and the ability of the virus to use such an environment to promote reverse transcription and thus protect itself from such destabilization.

ACKNOWLEDGMENTS

We thank Jeanine Bernaud for help with blood sample collection and the microscopy service of the IFR128 (Platim). We thank the AIDS Research and Reference Reagent Program of the NIH and J.-F. Mouscadet for material used in this study.

A.C. acknowledges the support of the CNRS. This study received the support of Sidaction, ANRS, and the NIH.

REFERENCES

1. **Aiken, C.** 1997. Pseudotyping human immunodeficiency virus type 1 (HIV-1) by the glycoprotein of vesicular stomatitis virus targets HIV-1 entry to an endocytic pathway and suppresses both the requirement for Nef and the sensitivity to cyclosporin A. J. Virol. **71:**5871–5877.
2. **Andreadis, S., T. Lavery, H. E. Davis, J. M. Le Doux, M. L. Yarmush, and J. R. Morgan.** 2000. Toward a more accurate quantitation of the activity of recombinant retroviruses: alternatives to titer and multiplicity of infection. J. Virol. **74:**3431–3439.
3. **Arfi, V., L. Riviere, L. Jarrosson-Wuilleme, C. Goujon, D. Rigal, J. L. Darlix, and A. Cimarelli.** 2008. Characterization of the early steps of infection of primary blood monocytes by human immunodeficiency virus type 1. J. Virol. **82:**6557–6565.
4. **Arhel, N., A. Genovesio, K. A. Kim, S. Miko, E. Perret, J. C. Olivo-Marin, S. Shorte, and P. Charneau.** 2006. Quantitative four-dimensional tracking of cytoplasmic and nuclear HIV-1 complexes. Nat. Methods **3:**817–824.
5. **Arhel, N. J., S. Souquere-Besse, S. Munier, P. Souque, S. Guadagnini, S. Rutherford, M. C. Prevost, T. D. Allen, and P. Charneau.** 2007. HIV-1 DNA Flap formation promotes uncoating of the pre-integration complex at the nuclear pore. EMBO J. **26:**3025–3037.
6. **Auewarakul, P., P. Wacharapornin, S. Srichatrapimuk, S. Chutipongtanate, and P. Puthavathana.** 2005. Uncoating of HIV-1 requires cellular activation. Virology **337:**93–101.
7. **Barbosa, P., P. Charneau, N. Dumey, and F. Clavel.** 1994. Kinetic analysis of HIV-1 early replicative steps in a coculture system. AIDS Res. Hum. Retrovir. **10:**53–59.
8. **Berger, G., C. Goujon, J. L. Darlix, and A. Cimarelli.** 2009. SIV(MAC) Vpx improves the transduction of dendritic cells with nonintegrative HIV-1-derived vectors. Gene Ther. **16:**159–163.
9. **Braaten, D., E. K. Franke, and J. Luban.** 1996. Cyclophilin A is required for an early step in the life cycle of human immunodeficiency virus type 1 before the initiation of reverse transcription. J. Virol. **70:**3551–3560.
10. **Brass, A. L., D. M. Dykxhoorn, Y. Benita, N. Yan, A. Engelman, R. J. Xavier, J. Lieberman, and S. J. Elledge.** 2008. Identification of host proteins required for HIV infection through a functional genomic screen. Science **319:**921–926.
11. **Bukrinskaya, A., B. Brichacek, A. Mann, and M. Stevenson.** 1998. Establishment of a functional human immunodeficiency virus type 1 (HIV-1) reverse transcription complex involves the cytoskeleton. J. Exp. Med. **188:** 2113–2125.
12. **Bukrinsky, M.** 2004. A hard way to the nucleus. Mol. Med. **10:**1–5.
13. **Bukrinsky, M. I., N. Sharova, M. P. Dempsey, T. L. Stanwick, A. G. Bukrinskaya, S. Haggerty, and M. Stevenson.** 1992. Active nuclear import of human immunodeficiency virus type 1 preintegration complexes. Proc. Natl. Acad. Sci. USA **89:**6580–6584.
14. **Chabes, A., and B. Stillman.** 2007. Constitutively high dNTP concentration inhibits cell cycle progression and the DNA damage checkpoint in yeast *Saccharomyces cerevisiae*. Proc. Natl. Acad. Sci. USA **104:**1183–1188.
15. **Collin, M., and S. Gordon.** 1994. The kinetics of human immunodeficiency virus reverse transcription are slower in primary human macrophages than in a lymphoid cell line. Virology **200:**114–120.

16. **Darlix, J. L., J. L. Garrido, N. Morellet, Y. Mely, and H. de Rocquigny.** 2007. Properties, functions, and drug targeting of the multifunctional nucleocapsid protein of the human immunodeficiency virus. Adv. Pharmacol. **55:**299–346.
17. **Gao, W. Y., A. Cara, R. C. Gallo, and F. Lori.** 1993. Low levels of deoxynucleotides in peripheral blood lymphocytes: a strategy to inhibit human immunodeficiency virus type 1 replication. Proc. Natl. Acad. Sci. USA **90:**8925–8928.
18. **Groschel, B., and F. Bushman.** 2005. Cell cycle arrest in G_2/M promotes early steps of infection by human immunodeficiency virus. J. Virol. **79:**5695–5704.
19. **Harris, D., N. Kaushik, P. K. Pandey, P. N. Yadav, and V. N. Pandey.** 1998. Functional analysis of amino acid residues constituting the dNTP binding pocket of HIV-1 reverse transcriptase. J. Biol. Chem. **273:**33624–33634.
20. **Hatziioannou, T., D. Perez-Caballero, S. Cowan, and P. D. Bieniasz.** 2005. Cyclophilin interactions with incoming human immunodeficiency virus type 1 capsids with opposing effects on infectivity in human cells. J. Virol. **79:**176–183.
21. **Iordanskiy, S., R. Berro, M. Altieri, F. Kashanchi, and M. Bukrinsky.** 2006. Intracytoplasmic maturation of the human immunodeficiency virus type 1 reverse transcription complexes determines their capacity to integrate into chromatin. Retrovirology. **3:**4.
22. **Jarrosson-Wuilleme, L., C. Goujon, J. Bernaud, D. Rigal, J. L. Darlix, and A. Cimarelli.** 2006. Transduction of nondividing human macrophages with gammaretrovirus-derived vectors. J. Virol. **80:**1152–1159.
23. **Kimpton, J., and M. Emerman.** 1992. Detection of replication-competent and pseudotyped human immunodeficiency virus with a sensitive cell line on the basis of activation of an integrated β-galactosidase gene. J. Virol. **66:**2232–2239.
24. **Koning, R., Y. Zhou, D. Elleder, T. L. Diamond, M. C. Bonamy, J. T. Irelan, C. Chiang, B. P. Tu, P. D. De Jesus, C. E. Lilley, S. Seidel, A. M. Opaluch, J. S. Caldwelll, M. D. Weitzman, K. L. Kuhen, S. Bandyopadhyay, T. Ideker, A. P. Orth, L. J. Miraglia, F. D. Bushman, J. A. Young, and S. K. Chanda.** 2008. Global analysis of host-pathogen interactions that regulate early-stage HIV-1 replication. Cell **135:**49–60.
25. **Korin, Y. D., and J. A. Zack.** 1999. Nonproductive human immunodeficiency virus type 1 infection in nucleoside-treated G0 lymphocytes. J. Virol. **73:**6526–6532.
26. **Korin, Y. D., and J. A. Zack.** 1998. Progression to the G1b phase of the cell cycle is required for completion of human immunodeficiency virus type 1 reverse transcription in T cells. J. Virol. **72:**3161–3168.
27. **Lin, Z. P., M. F. Belcourt, R. Carbone, J. S. Eaton, P. G. Penketh, G. S. Shadel, J. G. Cory, and A. C. Sartorelli.** 2007. Excess ribonucleotide reductase R2 subunits coordinate the S phase checkpoint to facilitate DNA damage repair and recovery from replication stress. Biochem. Pharmacol. **73:**760–772.
28. **Luban, J., K. L. Bossolt, E. K. Franke, G. V. Kalpana, and S. P. Goff.** 1993. Human immunodeficiency virus type 1 Gag protein binds to cyclophilins A and B. Cell **73:**1067–1078.
29. **Managlia, E. Z., A. Landay, and L. Al-Harthi.** 2006. Interleukin-7 induces HIV replication in primary naive T cells through a nuclear factor of activated T-cell (NFAT)-dependent pathway. Virology **350:**443–452.
30. **McDonald, D., M. A. Vodicka, G. Lucero, T. M. Svitkina, G. G. Borisy, M. Emerman, and T. J. Hope.** 2002. Visualization of the intracellular behavior of HIV in living cells. J. Cell Biol. **159:**441–452.
31. **Miller, M. D., C. M. Farnet, and F. D. Bushman.** 1997. Human immunodeficiency virus type 1 preintegration complexes: studies of organization and composition. J. Virol. **71:**5382–5390.
32. **Nakajima, N., R. Lu, and A. Engelman.** 2001. Human immunodeficiency virus type 1 replication in the absence of integrase-mediated dna recombination: definition of permissive and nonpermissive T-cell lines. J. Virol. **75:**7944–7955.
33. **Naldini, L., U. Blomer, P. Gallay, D. Ory, R. Mulligan, F. H. Gage, I. M. Verma, and D. Trono.** 1996. In vivo gene delivery and stable transduction of nondividing cells by a lentiviral vector. Science **272:**263–267.
34. **Nash, K. L., and A. M. Lever.** 2004. Green fluorescent protein: green cells do not always indicate gene expression. Gene Ther. **11:**882–883.
35. **Neil, S., F. Martin, Y. Ikeda, and M. Collins.** 2001. Postentry restriction to human immunodeficiency virus-based vector transduction in human monocytes. J. Virol. **75:**5448–5456.
36. **Nermut, M. V., and A. Fassati.** 2003. Structural analyses of purified human immunodeficiency virus type 1 intracellular reverse transcription complexes. J. Virol. **77:**8196–8206.
37. **Nisole, S., and A. Saib.** 2004. Early steps of retrovirus replicative cycle. Retrovirology **1:**9.
38. **O'Brien, W. A.** 1994. HIV-1 entry and reverse transcription in macrophages. J. Leukoc. Biol. **56:**273–277.
39. **O'Brien, W. A., A. Namazi, H. Kalhor, S. H. Mao, J. A. Zack, and I. S. Chen.** 1994. Kinetics of human immunodeficiency virus type 1 reverse transcription in blood mononuclear phagocytes are slowed by limitations of nucleotide precursors. J. Virol. **68:**1258–1263.
40. **Piatak, M., Jr., M. S. Saag, L. C. Yang, S. J. Clark, J. C. Kappes, K. C. Luk, B. H. Hahn, G. M. Shaw, and J. D. Lifson.** 1993. High levels of HIV-1 in plasma during all stages of infection determined by competitive PCR. Science **259:**1749–1754.
41. **Pierson, T. C., T. L. Kieffer, C. T. Ruff, C. Buck, S. J. Gange, and R. F. Siliciano.** 2002. Intrinsic stability of episomal circles formed during human immunodeficiency virus type 1 replication. J. Virol. **76:**4138–4144.
42. **Ravot, E., G. Comolli, F. Lori, and J. Lisziewicz.** 2002. High efficiency lentiviral gene delivery in non-dividing cells by deoxynucleoside treatment. J. Gene Med. **4:**161–169.
43. **Schwartz, O., V. Marechal, B. Friguet, F. Arenzana-Seisdedos, and J. M. Heard.** 1998. Antiviral activity of the proteasome on incoming human immunodeficiency virus type 1. J. Virol. **72:**3845–3850.
44. **Sokolskaja, E., D. M. Sayah, and J. Luban.** 2004. Target cell cyclophilin A modulates human immunodeficiency virus type 1 infectivity. J. Virol. **78:**12800–12808.
45. **Stremlau, M., M. Perron, M. Lee, Y. Li, B. Song, H. Javanbakht, F. Diaz-Griffero, D. J. Anderson, W. I. Sundquist, and J. Sodroski.** 2006. Specific recognition and accelerated uncoating of retroviral capsids by the TRIM5alpha restriction factor. Proc. Natl. Acad. Sci. USA **103:**5514–5519.
46. **Thomas, J. A., D. E. Ott, and R. J. Gorelick.** 2007. Efficiency of human immunodeficiency virus type 1 postentry infection processes: evidence against disproportionate numbers of defective virions. J. Virol. **81:**4367–4370.
47. **Towers, G. J., T. Hatziioannou, S. Cowan, S. P. Goff, J. Luban, and P. D. Bieniasz.** 2003. Cyclophilin A modulates the sensitivity of HIV-1 to host restriction factors. Nat. Med. **9:**1138–1143.
48. **Triques, K., and M. Stevenson.** 2004. Characterization of restrictions to human immunodeficiency virus type 1 infection of monocytes. J. Virol. **78:**5523–5527.
49. **Vandegraaff, N., R. Kumar, C. J. Burrell, and P. Li.** 2001. Kinetics of human immunodeficiency virus type 1 (HIV) DNA integration in acutely infected cells as determined using a novel assay for detection of integrated HIV DNA. J. Virol. **75:**11253–11260.
50. **Van Maele, B., J. De Rijck, E. De Clercq, and Z. Debyser.** 2003. Impact of the central polypurine tract on the kinetics of human immunodeficiency virus type 1 vector transduction. J. Virol. **77:**4685–4694.
51. **Vatakis, D. N., G. Bristol, T. A. Wilkinson, S. A. Chow, and J. A. Zack.** 2007. Immediate activation fails to rescue efficient human immunodeficiency virus replication in quiescent CD4+ T cells. J. Virol. **81:**3574–3582.
52. **Vatakis, D. N., C. C. Nixon, G. Bristol, and J. A. Zack.** 2009. Differentially stimulated $CD4^+$ T cells display altered HIV infection kinetics: implications for efficacy of antiviral agents. J. Virol. **83:**3374–3378.
53. **Yap, M. W., M. P. Dodding, and J. P. Stoye.** 2006. Trim-cyclophilin A fusion proteins can restrict human immunodeficiency virus type 1 infection at two distinct phases in the viral life cycle. J. Virol. **80:**4061–4067.
54. **Yin, L., D. Braaten, and J. Luban.** 1998. Human immunodeficiency virus type 1 replication is modulated by host cyclophilin A expression levels. J. Virol. **72:**6430–6436.
55. **Ylinen, L. M., T. Schaller, A. Price, A. J. Fletcher, M. Noursadeghi, L. C. James, and G. J. Towers.** 2009. Cyclophilin A levels dictate infection efficiency of human immunodeficiency virus type 1 capsid escape mutants A92E and G94D. J. Virol. **83:**2044–2047.
56. **Zack, J. A., S. J. Arrigo, S. R. Weitsman, A. S. Go, A. Haislip, and I. S. Chen.** 1990. HIV-1 entry into quiescent primary lymphocytes: molecular analysis reveals a labile, latent viral structure. Cell **61:**213–222.
57. **Zack, J. A., A. M. Haislip, P. Krogstad, and I. S. Chen.** 1992. Incompletely reverse-transcribed human immunodeficiency virus type 1 genomes in quiescent cells can function as intermediates in the retroviral life cycle. J. Virol. **66:**1717–1725.
58. **Zamborlini, A., J. Lehmann-Che, E. Clave, M. L. Giron, J. Tobaly-Tapiero, P. Roingeard, S. Emiliani, A. Toubert, H. de The, and A. Saib.** 2007. Centrosomal pre-integration latency of HIV-1 in quiescent cells. Retrovirology 4:63.
59. **Zhang, H., G. Dornadula, J. Orenstein, and R. J. Pomerantz.** 2000. Morphologic changes in human immunodeficiency virus type 1 virions secondary to intravirion reverse transcription: evidence indicating that reverse transcription may not take place within the intact viral core. J. Hum. Virol. **3:**165–172.
60. **Zhang, H., G. Dornadula, and R. J. Pomerantz.** 1996. Endogenous reverse transcription of human immunodeficiency virus type 1 in physiological microenviroments: an important stage for viral infection of nondividing cells. J. Virol. **70:**2809–2824.
61. **Zhou, Y., H. Zhang, J. D. Siliciano, and R. F. Siliciano.** 2005. Kinetics of human immunodeficiency virus type 1 decay following entry into resting $CD4^+$ T cells. J. Virol. **79:**2199–2210.